J. Plasma Phys. (2015), *vol.* 81, 495810603 © Cambridge University Press 2015
doi:10.1017/S0022377815001130

Integrodifferential models of electron transport for negative ion sources

Marco Cavenago†

INFN-LNL, Lab. Nazionali Legnaro, Accelerator division, v.le dell'Università n. 2, I-35020, Legnaro (PD), Italy

(Received 7 April 2015; revised 18 September 2015; accepted 18 September 2015)

Thanks to the presence of a transverse magnetic flux density (B_x and B_y where z is the extraction axis), the undesired extraction of electrons from a negative ion source is reduced and it is due to collisions. The electron transport is studied with a kinetic model, including Vlasov–Poisson effects and atomic collisions. The integrodifferential equations (IDE) resulting from a reduction to a one-dimensional problem (1-D) by integration on characteristic orbits are strongly affected by the trapped orbits, as here evaluated; a kernel calculation with a partial wave approximation is introduced. Dependencies from the local drift velocity v_d and effective Larmor radius L_e are found. Solutions are investigated in simple cases with a constant electron current (no additional electron production). Equilibrium solution and electron conductivity are analytically obtained. Presheath solutions are discussed; the approximated conversion to differential equations that are adequate for presheath only (with moderated electric field gradient $E_{z,z} > -eB_x^2/m$) and their numeric solutions coupled to Poisson equation are reported, and compared to iterative IDE solutions. Examples with different values of L_e and mean free path (mfp) ratio are described.

1. Introduction

In negative ion plasma sources, the design of the extraction system must consider a possibly large current density of electrons j_e, which are co-extracted with the ions, H^- for example. A transverse magnetic field is applied to reduce the ratio R_j of j_e and the ion current density j_{H^-} so that collisional effects needs to be modelled before any R_j optimization. While the complete physics is overwhelmingly complex and 3-D in space, here we present a 1-D kinetic model of electron transport which retains the main effects of the collisions and magnetic field accounted for by adequate integrals, calculated in detail from a kinetic equation with a simple collisional term.

Use of integrodifferential equations (Morse & Feshbach 1953), even if less common than PDE (partial differential equation) and ODE (ordinary differential equation) in source modelling, is necessary when kinetic effects are projected to spatial coordinates, as indicated by a classic model (Tonks & Langmuir 1929), where electric field component E_z and ion production and motion along z were included in the 'complete plasma–sheath equation'. Its solutions, numerically obtained by (Self 1963), have no singularities at the plasma–sheath interface; its approximations, namely the plasma

† Email address for correspondence: cavenago@lnl.infn.it

https://doi.org/10.1017/S0022377815001130 Published online by Cambridge University Press

equation (neglecting Poisson's equation) and the sheath equation (neglecting details of the kinetic effects) have singularities at the joining interface. Among a vast literature and reviews (Lieberman & Lichtenberg 1994; Forrester 1996; Brown 2004), we note other classical papers on two length scales joining (Caruso & Cavaliere 1962), fluid models (Hutchinson 1987; Franklin 2003), Bohm speed (Riemann 1991) and sheath singularity matching (Benilov 2009). Additional physical information is presented in other fluid models (Chodura 1982) and integrodifferential kinetic models, with no magnetic field (Emmert *et al.* 1980), zero speed after collision (Schmitz, Riemann & Daube 1996) or with linearized kinetic equations (Dikman & Meierovich 1973), in several numerical simulation papers (Takado, Miyamoto & Hatayama 2004; Taccogna *et al.* 2008; Mochalskyy, Lifschitz & Minea 2010; Taccogna, Minelli & Longo 2013).

In our model, the temperature of the electrons, protons and H^- is assumed equal to T_0 (in energy units), particle densities (for example electron density n_e) are divided by a reference density N_0 (so that $n_a = n_e/N_0$ is dimensionless), momenta are divided by $\sqrt{mT_0}$ and similarly for velocities and particle flow density $j = -j_e/eN_0v_{th}$ with $v_{th} = \sqrt{T_0/m}$. For simplicity, here we discuss only electron transport with a kinetic model; H^- transport may be similarly described (Cavenago 2008) or with a fluid model (Cavenago 2010); protons are described with a Maxwellian equilibrium or, when recombination with H^- is included, with a fluid model (Cavenago 2010). Particle net flow density $j = j^{fo} - j^b$ can be separated in forward flow j^{fo} and backward flow j^b (here for convention $j^b \geqslant 0$ as well as $j^{fo} \geqslant 0$); averaged absolute value is defined as $j_a = (j^{fo} + j^b)/2$; see before (2.4) for detail.

The rest of the paper is organized as follows. In § 2, from the kinetic equation, we will derive the integrodifferential equation system

$$\frac{\partial j_a(z)}{\partial z} = -\frac{j}{2\lambda} + \int \mathrm{d}z_2\, K(z_2 - z; z)\frac{2j_a(z_2)}{\lambda}, \tag{1.1}$$

$$n_a(z) = \int \mathrm{d}z_2\, N(z_2 - z; z)\frac{2j_a(z_2)}{\lambda}, \tag{1.2}$$

where λ is the mfp and the K and N expressions include the recirculation effect due to the magnetic field; we also introduce the effective Larmor radius L_e and related parameters. In § 3 the phase space, integrals in K and N are calculated, introducing accurate approximations, when needed (see also appendices A and B). In § 4, self-consistent solutions of (1.1) and (1.2) and the Poisson equation are discussed, both in steady state (zero electric field gradient $E_{z,z} = 0$) and in the presheath, where gradients are small. Presheath solutions are approximated with reliable ODE numerical tools (Wolfram 2003) and a regularization technique; then they are refined with an iterative procedure. All of these solutions confirm that a quiet quasi-neutral plasma presheath for $z \to -\infty$ may match to an increasing field E_z for positive z, as in the sheath solution.

2. Stationary model basic equations

Let $v(z) = -e\phi/T_0$ and $a(z) = -eA_y/\sqrt{mT_0}$, with ϕ the electric potential and $(0, A_y, 0)$ the vector potential; we assume no variations along x and y (1-D model) and time. The scaled Hamiltonian H/T_0 is

$$h(z, p_z; P_y) = \tfrac{1}{2}p_z^2 + \tfrac{1}{2}(P_y - a(z))^2 + v(z), \tag{2.1}$$

where P_y is a canonical momentum component and is conserved (except for collisions); mechanical momentum is $p_y = P_y - a(z)$. In notation here, semicolon(s)

https://doi.org/10.1017/S0022377815001130 Published online by Cambridge University Press

separate blocks of function arguments, which can be omitted for brevity or transformed; moreover we use $\partial_x b = b_{,x}$ as shorthand for the partial x-derivative of b and also $b'(x)$ for the ordinary derivative. The phase-space density $f(z, p_z, P_y)$ of each species (integrated on p_x) satisfies a kinetic equation

$$p_z f_{,z} - h_{,z} f_{,p_z} = \mathcal{S} + \mathcal{C}, \tag{2.2}$$

where $\mathcal{S}$ is the source term and $\mathcal{C}$ is the collisional term (in scaled variables); when $\mathcal{S} = \mathcal{C} = 0$ we have the Vlasov equation. Let λ_a be the attenuation length (due to recombination with protons, ionization of H^- ions or attachment of the electrons to H_2) and let λ_i be the mfp including any other collisions (elastic and inelastic, mainly with gas of density n_g). A reasonably simple approximation for $\mathcal{C}$ is a fixed inelastic scatterer 1-D model:

$$\mathcal{C} = |p_z| \left\{ -\frac{f}{\lambda_t} + \frac{f_g(p_z) f_g(p_y)}{c_\pi \lambda_i} \int' |p_z| f \right\}, \quad \frac{1}{\lambda_t} = \frac{1}{\lambda_i} + \frac{1}{\lambda_a}, \tag{2.3}$$

with $\int' = \int \mathrm{d}p_z \, \mathrm{d}P_y$, the Gaussian factor $f_g(x) = \exp(-x^2/2)/(2\pi)^{1/2}$ and $c_\pi = \sqrt{2/\pi}$.

In the model discussed here, the mfp λ_i is taken as a constant parameter; it may be argued that other cases must be considered, as for example a constant collision frequency ν_m, often used (Lieberman & Lichtenberg 1994), or a Coulomb collision case, where $\nu_m \propto p^{-3}$ with a large reduction due to the low ionization degree of H^- source plasmas (order of $n_e/n_g = 0.001$). A detailed comparison of these terms is beyond the scope of this paper, due to the increase in labour and/or the approximations required by the kinetic calculations in these cases, and is worth future investigation. The motivations for the (2.3) model assumption are the possibility of considering λ as a parameter to be adjusted (to real atomic physics cross sections), and the simplicity of orbit integration in this model.

Furthermore, we neglect λ_a^{-1} and $\mathcal{S}$ in the following, so that $\lambda_t = \lambda_i = \lambda$. With these assumptions, applying $\int'$ to the kinetic equation (2.2) gives simply the net flow conservation $j_{,z} = 0$. Forward and backward particle flows are defined as $j^{fo} = \int' p_z f \Theta(p_z)$ and $j^b = -\int' p_z f \Theta(-p_z)$ with the Heaviside function $\Theta(x)$; note that $\Theta(0) = 1$. We have $j^{fo} = j_a + j/2$. Applying $\int' \Theta(p_z)$ to the kinetic equation, we obtain

$$j_{a,z}(z) = j^{fo}_{,z} = -\frac{1}{2}(j/\lambda) - \int \mathrm{d}P_y \, h_{,z} f(z, 0, P_y). \tag{2.4}$$

2.1. *Reversal points of each orbit*

Let P_y^D be the value of P^y corresponding to a trajectory with z constant (called an equilibrium orbit). From the Hamilton equations, we have

$$P_y^D(z) = a(z) + \{v_{,z}(z)/a_{,z}(z)\}, \tag{2.5}$$

which defines a $P_y^D(z)$ function; moreover the function of z equal to $v_D(z) \equiv P_y^D - a(z) = p_y = v_{,z}(z)/a_{,z}(z)$ is also the drift velocity for this equilibrium orbit.

For a generic orbit γ, the $p_z = 0$ points are called reversal points, with a maximum of two points, z^- and z^+, with $z^- \leqslant z^+$, see figure 1; orbits with one only reversal point correspond to extracted electrons (with z^- finite and $z^+ \to +\infty$) or to electrons lost into the plasma (with z^+ finite and $z^- \to -\infty$). Orbits with no reversal points,

https://doi.org/10.1017/S0022377815001130 Published online by Cambridge University Press

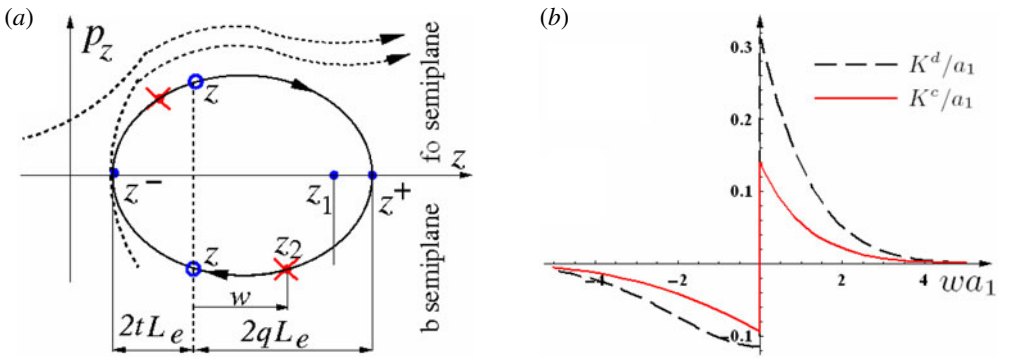


FIGURE 1. (*a*) A closed orbit in the zp_z plane, with observation points z (open circles) and collision points (crosses); note $w = 2L_e q_0$ and other coordinates q and t and open orbits are shown by the dashed lines; (*b*) the kernel parts, direct K^d/a_1 and circulating K^c/a_1 versus wa_1, in the case $v_1/a_1 = -0.4$, $v_2/a_1^2 = -0.2$ and $a_1\lambda = 2.5$ (which gives $c_d = 1$).

possible in regions with negligible magnetic field or in small sources, are discussed elsewhere (Cavenago 2008).

Reversal points divide an orbit into two arcs, the forward arc γ^{fo} with $p_z \geqslant 0$ and the backward arc γ^b with $p_z \leqslant 0$. The quantity $p = p_y - v_D(z) = P_y - P_y^D$ oscillates as z does along an orbit, but its value p^- at z^-, that is $p^- = P_y - P_y^D(z^-)$, is a gauge invariant constant of motion and is a measure of deviation from equilibrium orbit; similarly for $p^+ = P_y - P_y^D(z^+)$, which is not independent of p^-.

Let (η_z, η_y) be the values of (p_z, p_y) just after a collision at point z_2, and h_2 be the Hamiltonian at this orbit point. We relate η_y to p_y at an observation point z by

$$p + v_D(z) = p_y = P_y - a(z) = P_y - a(z_2) - \bar{a} = \eta_y - \bar{a}, \tag{2.6}$$

with the shorthand for the potential differences $\bar{a} = a(z) - a(z_2)$ and $\bar{v} = v(z) - v(z_2)$. Since $h_2 = h$ we also have $\eta_z = \pm\sqrt{p_z^2 + 2V_e}$ with the effective potential

$$V_e(z, z_2, p) = h_2 - \frac{\eta_y^2 + p_z^2}{2} - v(z_2) = \bar{v} + \frac{1}{2}\bar{a}^2 - \bar{a}\eta_y = \bar{v} - \frac{1}{2}\bar{a}^2 - \bar{a}(p + v_D(z)). \tag{2.7}$$

2.2. *Integration of the kinetic equation on orbits*

Integrating equation (2.2) along an orbit arc (for example the forward arc), from point z_1 to point z for $p_z \geqslant 0$, we obtain

$$f(z, p_z, P_y) = f(z_1, p_z^\gamma, P_y)\mathrm{e}^{-(|z_1 - z|)/\lambda} + \int_{z_1}^{z} \mathrm{d}z_2\, \mathrm{e}^{-(|z - z_2|)/\lambda}\frac{2j_a(z_2)}{\lambda}G^\gamma, \tag{2.8}$$

with $z \geqslant z_2 \geqslant z_1 \geqslant z^-$ and $p_z^\gamma = p_z$ at z_1 determined by the orbit; the scattering factor

$$G^\gamma \equiv \frac{f_g(\eta_z)f_g(\eta_y)}{c_\pi} = \frac{\mathrm{e}^{v(z_2) - h_2}}{2\sqrt{2\pi}} = \frac{\mathrm{e}^{-\bar{v} - (1/2)(p_z^2 + p_y^2)}}{2\sqrt{2\pi}}\theta_C = G(z, p_z, P_y; z_2), \tag{2.9}$$

can be transformed from a function of η_z, η_y to a function of $\boldsymbol{p}$, z and z_2 as shown, thanks to the $h = h_2$ energy conservation, represented by the factor θ_C, equal to

https://doi.org/10.1017/S0022377815001130 Published online by Cambridge University Press

zero when $z, \boldsymbol{p}$ and $z_2, \boldsymbol{\eta}$ are not on the same orbit and equal to one if they are. A convenient formula is $\theta_C = \Theta(p_z^2 + 2V_e)\Theta(z_2 - z^-)\Theta(z^+ - z_2)$. The expression for f on the backward arc is similar to (2.8), with $z \leqslant z_2 \leqslant z_1 \leqslant z^+$, the integration limits reversed and the same G, since G is even in p_z. For $z_1 = z^+$ we obtain

$$f(z, p_z \leqslant 0, P_y) = f(z^+, 0, P_y)\mathrm{e}^{(z-z^+)/\lambda} + \int_z^{z^+} \mathrm{d}z_2\, \mathrm{e}^{(z-z_2)/\lambda} \frac{2j_a(z_2)}{\lambda} G^\gamma. \tag{2.10}$$

2.3. *The recirculation effect*

When an orbit has two reversal points, which is the most common case in sources much larger than the Larmor radius, the orbit is closed and electrons may recirculate from z^- to z^+ and vice versa, if not scattered during travel. Using (2.8) in the case $z = z^+$ and $z_1 = z^-$ we find:

$$f(z^+, 0, P_y) = f(z^-, 0, P_y)\mathrm{e}^{-s_d} + \int_{z^-}^{z^+} \mathrm{d}z_2\, \mathrm{e}^{(z_2-z^+)/\lambda} G(z^+, 0, P_y; z_2) \frac{2j_a(z_2)}{\lambda}, \tag{2.11}$$

with $s_d = (z^+ - z^-)/\lambda$. Similarly substituting $z = z^-$ in (2.10) for the $p_z \leqslant 0$ arc,

$$f(z^-, 0, P_y) = f(z^+, 0, P_y)\mathrm{e}^{-s_d} + \int_{z^-}^{z^+} \mathrm{d}z_2\, \mathrm{e}^{(z^- - z_2)/\lambda} G(z^-, 0, P_y; z_2) \frac{2j_a(z_2)}{\lambda}. \tag{2.12}$$

For any fixed z_2, we can apply (2.9) twice, once with $z = z^-$ and the other time with $z = z^+$, so proving the equalities

$$G^\gamma = G(z^-, 0, P_y; z_2) = G(z^+, 0, P_y; z_2) = \tfrac{1}{2}\theta_C \mathrm{e}^{v(z_2) - v(z^\pm)} f_g(p^\pm + v_D(z^\pm)), \tag{2.13}$$

since $p_z = 0$ at reversal points and p_y may be expressed with (2.6). Solving the (2.11) and (2.12) system for $f(z^\pm, 0, P_y)$ and rearranging we obtain

$$f(z^-, 0, P_y) = \frac{2}{\lambda} \int_{z^-}^{z^+} \mathrm{d}z_2\, R^- G^\gamma j_a(z_2), \quad f(z^+, 0, P_y) = \frac{2}{\lambda} \int_{z^-}^{z^+} \mathrm{d}z_2\, R^+ G^\gamma j_a(z_2), \tag{2.14a,b}$$

with the response factors

$$R^+ = \frac{\cosh((z_2 - z^-)/\lambda)}{\sinh s_d}, \quad R^- = \frac{\cosh((z_2 - z^+)/\lambda)}{\sinh s_d}. \tag{2.15a,b}$$

We may rewrite these as $R^- = R(z^- - z_2)$ and $R^+ = R(z^+ - z_2)$ with the response function

$$R(x) = \exp\left(-\frac{|x|}{\lambda}\right) + \cosh\left(\frac{x}{\lambda}\right) \frac{\mathrm{e}^{-s_d}}{\sinh s_d}. \tag{2.16}$$

Let R^d be the first term above and R^c the second term. Note that R^d is the expression obtained neglecting recirculation (Cavenago 2008). For $\lambda \to 0$, with $z^+ - z^-$ fixed, we have $s_d \to \infty$ and R/R^d converges to 1. Thus R^d is the no-recirculation response (or direct response) and R^c expresses the additional effect of recirculation, which has a pole for $\lambda \to \infty$ (cancelled by the $2/\lambda$ factor in (2.14)), as expected.

https://doi.org/10.1017/S0022377815001130 Published online by Cambridge University Press

2.4. *The kernel K*

The Lorentz force is $-h_{,z} = p\, a_{,z}$ thanks to (2.6). With no loss of generality, we assume $a_{,z} > 0$; so we have $p > 0$ at a z^- point (since it is a minimum of z on the orbit), and $p < 0$ at a z^+ point. We now substitute (2.14) into (2.4), changing the integration variable from P_y to p; since (2.13) and (2.16) hold, exchanging p and z_2 integrations we find (1.1) with a kernel

$$K(z_2 - z; z; a, v) = \frac{1}{2} a_{,z} \mathrm{e}^{v(z_2)-v(z)} \int_{-\infty}^{\infty} \mathrm{d}p\, \theta_C^0 R(z - z_2) p f_g(p + v_D(z)), \tag{2.17}$$

where θ_C^0 is θ_C at $p_z = 0$; this factor implicitly selects the p integration domain D^1 according to the (2.14) integration limits. It is convenient to introduce the quantity $w = z_2 - z$ to compute the domain $D_w^1(p)$, as detailed in appendix A, with results:

$$D_w^1(p) = \{s_w p \geqslant \max(0, s_w q_0)\}, \quad q_0(w) = (\bar{v}/\bar{a}) - \tfrac{1}{2}\bar{a} - v_d, \tag{2.18a,b}$$

where we introduced the shorthand $s_w = \mathrm{sign}(w)$ and $v_d = v_D(z)$. For example, at any fixed z the local second-order approximation is defined by:

$$v(z + w) = v_0 + v_1 w + \tfrac{1}{2} v_2 w^2 + O(w)^3, \quad a(z + w) \cong a_0 + a_1 w + O(w)^3, \tag{2.19a,b}$$

where the variations of the coefficients a_1 and $v_2 = v''(z)$ are assumed zero or adiabatically slow with z with respect to the fast oscillations of orbit with w; note $a_1 = a'(z) > 0$ and $a_2 = 0$. We have $v_d = v_1/a_1$ and $q_0(w) = w/(2L_e)$ with $L_e = a_1/(a_1^2 + v_2)$ an effective Larmor radius. Also it results in $z^+ - z^- = 2L_e|p^-|$ and $p^+ = -p^-$, which clearly shows that the oscillation width is $2L_e$ for $p = 1$. In this example, when $v_2 + a_1^2 > 0$ all orbits are closed and the integration domain D^1 is simply $p/w \geqslant 1/(2L_e)$. When $v_2 + a_1^2 < 0$, the effective Larmor radius is negative, indicating instability of the equilibrium orbit, and the domain D^1 is simply $p/w \geqslant 0$.

2.5. *The kernel N*

We calculate first n_a^b, that is the density due to backward moving particles: $n_a^b = \int' f \Theta(-p_z) = (2/\lambda) \int \mathrm{d}z_2\, N^b j_a$ with the kernel part N^b. Then we will use symmetry to calculate the density contribution of the forward flow: $n_a^{fo} = \int' f \Theta(p_z) = (2/\lambda) \int \mathrm{d}z_2\, N^{fo} j_a$, where N^{fo} is the other part of the kernel N. We consider all orbits closed. Using f value from (2.10) and exchanging the order of integration, we find

$$N^b(w; z; a, v) = \int \mathrm{d}p_y \int_{-\infty}^{0} \mathrm{d}p_z [\mathrm{e}^{-w/\lambda} \Theta(w) + \mathrm{e}^{-w^+/\lambda} R(w^+ - w)] G(z, p_z, P_y; z + w), \tag{2.20}$$

with the shorthand $w^+ = z^+ - z$ and $w^- = z^- - z$ and integration domain restricted by the θ_C factor in G. Transformation from p_y, p_z to quantities

$$q = \tfrac{1}{2}(p - p^+), \quad t = \tfrac{1}{2}(p^- - p), \tag{2.21a,b}$$

(where t from this point is not the time) is useful for calculating N^b, at least with (2.19) potential; transformation and domains $D_w^2(q, t)$ and $D_w^3(p_z, p_y)$ are calculated in

https://doi.org/10.1017/S0022377815001130 Published online by Cambridge University Press

(A 3), (A 4) and (A 6). Expanding G, note that N^b can be factorized as $N^b = k_a \mathrm{e}^{-\bar{v}} \check{N}^b$ with

$$\check{N}^b(w;\, c_1,\, v_d,\, c_d) = \int_{D_w^2} \mathrm{d}q\, \mathrm{d}t \frac{q+t}{\sqrt{qt}} [\mathrm{e}^{-c_d q_0} \Theta(w) + \mathrm{e}^{-c_d q} R(c_d(q-q_0))] E_1, \tag{2.22}$$

where $E_1 = \mathrm{e}^{-\frac{1}{2}(q^2+t^2+v_d^2)-c_1 qt - v_d(q-t)}$ and $k_a = ((L_e a_1/2\pi)^{1/2})/2$; the dependence on a and v is now expressed by the parameters $c_1 = 2L_e a_1 - 1$, v_d and $c_d = 2L_e/\lambda$. The integral for N^{fo} is as (2.22), but with t instead of q in the square bracket factor. The symmetry S_1 sends w into $-w$ and v_d into $-v_d$ as explained at the end of appendix A and the domain change due to symmetry is equivalent to the exchange of q and t in the integral above; so we have

$$N^{fo} = k_a \mathrm{e}^{-\bar{v}} \check{N}^{fo}, \quad \check{N}^{fo}(w;\, c_1,\, v_d,\, c_d) = \check{N}^b(-w;\, c_1,\, -v_d,\, c_d). \tag{2.23a,b}$$

3. Kernels and damped partial waves

In this section, we simplify the kernel N calculation and give approximated analytic results for the kernel K, developing a common approach for both.

For simplicity, we consider (2.19) potentials. Note that the non-recirculating part K^d can be exactly calculated and is proportional to the $\mathrm{e}^{-|z-z_2|/\lambda} M_{,z}$ calculated for more general examples elsewhere (Cavenago 2008), while the non-recirculating part of N corresponds to $\mathrm{e}^{-|z-z_2|/\lambda} N$ there. To approximate K^c we note first the tight upper bound $b_2(x)$ of

$$b(x) = x\mathrm{e}^{-x}/\sinh x \leqslant 2x\mathrm{e}^{-2x} + \mathrm{e}^{-3x} \equiv b_2(x) \tag{3.1}$$

for $0 \leqslant x \leqslant \infty$. The so-called damped partial waves e^{-2x} and e^{-3x} will make analytic calculations possible, and notwithstanding that we use only two terms, we obtain a good approximation for the whole range discussed. Replacing $b(c_d p)$ with $b_2(c_d p)$ in (2.17), K becomes the sum of five terms of the form $\hat{K}^i_{n;k}$ defined as

$$\hat{K}^i_{n;k}(q_0,\, v_d,\, c_d) = \frac{1}{2} \mathrm{sign}(q_0) \mathrm{e}^{-ic_d|q_0|} \int_{|q_0|}^{\infty} \mathrm{d}p\, p^n \mathrm{e}^{-kc_d p} f_g(ps_0 + v_d), \tag{3.2}$$

with $s_0 = \mathrm{sign}(q_0)$, typical values of indexes $n = 0,\, 1$, $i = \pm 1$ and $k = 0,\, 2,\, 3$; where the index separator ';' is usually dropped. In detail, $K = K^d + K^c$ and

$$K^d(w;\, z;\, v_d,\, c_d) = a_{,z} \mathrm{e}^{-\bar{v}} \hat{K}^1_{10}(w/2L_e,\, v_d,\, c_d), \tag{3.3}$$

$$K^c \cong a_{,z} \mathrm{e}^{-\bar{v}} \left[\hat{K}^1_{12}\left(\frac{w}{2L_e},\, v_d,\, c_d\right) + \hat{K}^{-1}_{12} + \frac{\hat{K}^1_{03} + \hat{K}^{-1}_{03}}{2c_d} \right], \tag{3.4}$$

where we omit repeated arguments after the first term. An auxiliary integral, here defined for $t_0 \geqslant 0$ and for any s as

$$f_n(t_0,\, s) = \int_{t_0}^{\infty} \mathrm{d}t\, t^{n-(1/2)} \mathrm{e}^{-ts-(1/2)t^2}, \tag{3.5}$$

whose exact values are listed in appendix B when known, is convenient to express $\hat{K}$, and it also helps for $\check{N}$. For $q_0 \geqslant 0$ we can write

$$\hat{K}^i_{nk}(q_0,\, v_d,\, c_d) = \tfrac{1}{2} \mathrm{e}^{-ic_d q_0} f_g(v_d) f_{n+(1/2)}(q_0,\, v_d + kc_d), \tag{3.6}$$

https://doi.org/10.1017/S0022377815001130 Published online by Cambridge University Press

with $f_{n+(1/2)}$ given by (B 3) in terms of the complementary error function $\mathrm{erfc}(x) = 1 - \mathrm{erf}(x)$; for $q_0 < 0$ the symmetry property $\hat{K}^i_{nk}(q_0, v_d, c_d) = -\hat{K}^i_{nk}(-q_0, -v_d, c_d)$ is used. Note that $\hat{K}$ is discontinuous at $q_0 = 0$, see figure 1(*b*); the pole of c_d was previously discussed. From (B 5) we see that $\hat{K}^i_{nk}$ is asymptotically bounded by $\exp[-(i+k)|q_0|c_d]$ for large w (with a strong safety factor $\mathrm{e}^{-q_0^2/2}$), so the $i = -1$ effect is dominated by $k = 2$ and K^{-1}_{12} is as damped as K^1_{10}.

3.1. *Calculation of density kernel N*

To exploit the partial waves formula (3.1), we define the density terms

$$\hat{N}^i_{nk;m}(q_0; c_1, v_d, c_d) = \mathrm{e}^{ic_d q_0} \int_{D^2_w} \mathrm{d}q\,\mathrm{d}t \frac{(q+t)^n}{\sqrt{qt}} E_1 \mathrm{e}^{-kc_d(q+t) - mc_d(q-t)}, \tag{3.7}$$

with E_1 given after (2.22); from it, the kernel part $\check{N}^b$, thanks to (3.1) and (A 5), becomes

$$\check{N}^b(w, c_1, v_d, c_d) \cong \Theta(w)\hat{N}^{-1}_{10;0} + \hat{N}^{-1}_{12;0} + \hat{N}^1_{11;1} + \hat{N}^1_{13;1} + \frac{\hat{N}^{-1}_{03;0} + \hat{N}^1_{04;1}}{2c_d}, \tag{3.8}$$

where all density terms are evaluated at $q_0 = w/2L_e$, c_1, v_d, c_d. The symmetry relation for $\hat{N}$ is

$$\hat{N}^i_{nk;m}(-q_0, c_1, v_d, c_d) = \hat{N}^{-i}_{nk;-m}(q_0, c_1, -v_d, c_d). \tag{3.9}$$

Therefore, in the total density kernel (backward plus forward parts)

$$\begin{aligned} N(w; z; c_1, v_d, c_d) \;=\; & k_a \mathrm{e}^{-\bar{v}} [\hat{N}^{-s_w}_{10;0} + \hat{N}^{-1}_{12;0} + N^1_{12;0} + \hat{N}^{-1}_{11;-1} + \hat{N}^1_{11;1} \\ & + \hat{N}^{-1}_{13;-1} + \hat{N}^1_{13;1} + (2c_d)^{-1}(\hat{N}^{-1}_{03;0} + \hat{N}^1_{03;0} + \hat{N}^{-1}_{04;-1} + \hat{N}^1_{04;1})] \end{aligned} \tag{3.10}$$

all density terms $\hat{N}$ are evaluated at $q_0 = w/2L_e$, c_1, v_d, c_d (one change of sign of v_d from $\check{N}^b$ to $\check{N}^{fo}$ thanks to (2.23) and another change applying (3.9)); the first term, with $s_w = \mathrm{sign}(w)$, includes the first terms of $\check{N}^b$ and of $\check{N}^{fo}$.

In (3.7), for $q_0 \geqslant 0$ the integration on t runs from 0 to ∞ so it can be performed analytically with (3.5), obtaining an intermediate computation step:

$$\hat{N}^i_{nk;m}(q_0; c_1, v_d, c_d) = \mathrm{e}^{ic_d q_0 - (v_d^2/2)} \int_{q_0}^{\infty} \mathrm{d}q\, \mathrm{e}^{-qs^+ - (q^2/2)} g_n(c_1 q + s^-, q), \tag{3.11}$$

with the shorthand $s^- = (k-m)c_d - v_d$ and $s^+ = (k+m)c_d + v_d$; the functions $g_0(x, q) = f_0(0, x)$ and $g_1(x, q) = f_1(0, x) + q f_0(0, x)$ are given by (B 4); in general the integration of q should be obtained numerically. For $q_0 < 0$, the symmetry relation is used. For $q_0 = 0$ and $c_1 = 1$ a good approximation is reported in (B 6).

3.2. *Moments of the kernels K and N*

Since K has positive and negative values, initial information on its effect is given by $\int \mathrm{d}w\, K$, or in general by the ℓth moment $\mathcal{K}_\ell = \int \mathrm{d}w\, K w^\ell/\ell!$ with integer $\ell \geqslant 0$. We first calculate the integral moments term by term in the $w > 0$ range

$${}^+\hat{\mathcal{K}}^{\ell i}_{nk}(v_d, c_d) = a_1 \int_0^{\infty} \mathrm{d}w\, \mathrm{e}^{-\bar{v}} \frac{w^\ell}{\ell!} \hat{K}^i_{nk}\left(\frac{w}{2L_e}, v_d, c_d\right); \tag{3.12}$$

https://doi.org/10.1017/S0022377815001130 Published online by Cambridge University Press

the similar integral ${}^{-}\hat{\mathcal{K}}^{\ell i}_{nk}$ on the $w<0$ range satisfies the symmetry property

$$ {}^{-}\hat{\mathcal{K}}^{\ell i}_{nk}(v_d, c_d) = (-1)^{\ell+1} \times {}^{+}\hat{\mathcal{K}}^{\ell i}_{nk}(-v_d, c_d); \tag{3.13} $$

their sum is $\hat{\mathcal{K}}^{\ell i}_{nk} \equiv {}^{-}\hat{\mathcal{K}}^{\ell i}_{nk} + {}^{+}\hat{\mathcal{K}}^{\ell i}_{nk}$. Exact calculation is possible in the $v_2 = 0$ case (that is $c_1 = 1$): first by changing the integration variable to $y = w/2L_e$ we obtain

$$ {}^{+}\hat{\mathcal{K}}^{\ell i}_{nk} = a_1 (2L_e)^{\ell+1} \int_0^\infty \mathrm{d}y\, \mathrm{e}^{-c_y y} y^\ell \int_y^\infty \mathrm{d}p\, \frac{1}{2} p^n \mathrm{e}^{-kc_d p} f_g(p + v_d)/\ell!, \tag{3.14} $$

with $c_y = ic_d - 2L_e a_1 v_d$. Exchanging the y and p integration order, the integration on y is elementary and gives

$$ \int_0^p \mathrm{d}y \frac{y^\ell}{\ell!} \exp(-c_y y) = c_y^{-\ell-1} \left[1 - \mathrm{e}^{-c_y p} \sum_{\nu=0}^{\nu=\ell} \frac{(c_y p)^\nu}{\nu!} \right]. \tag{3.15} $$

Now we define the value $\tilde{k}(c_y) = k + (c_y/c_d)$, which is real since $c_d > 0$, while the index k was an integer; note that the $\hat{K}^0_{n;\tilde{k}}(0, v_d, c_d)$ integrand contains a factor $\mathrm{e}^{-c_y p - kc_d p}$ and the same factor appears by substituting (3.15) into (3.14). This allows us to write ${}^{+}\hat{\mathcal{K}}^{\ell i}_{nk}$ with known functions

$$ {}^{+}\hat{\mathcal{K}}^{\ell i}_{nk} = a_1 \left(\frac{2L_e}{c_y} \right)^{\ell+1} \left[\hat{K}^0_{nk}(0, v_d, c_d) - \sum_{\nu=0}^{\nu=\ell} \frac{(-c_y)^\nu}{\nu!} \mathcal{O}_c{}^\nu \hat{K}^0_{n;\tilde{k}(c_y)}(0, v_d, c_d) \right], \tag{3.16} $$

with the differential operator $\mathcal{O}_c \equiv \partial/\partial c_y$. For example

$$ {}^{+}\hat{\mathcal{K}}^{1i}_{nk}(v_d, c_d) = a_1 (2L_e/c_y)^2 [\hat{K}^0_{nk}(0, v_d, c_d) - \hat{K}^0_{n;\tilde{k}}(0, v_d, c_d) - c_y \hat{K}^0_{n+1;\tilde{k}}]. \tag{3.17} $$

Moments $\mathcal{K}_\ell = \int \mathrm{d}w\, K w^\ell/\ell!$ simply correspond to the sum of the terms from (3.4) and (3.3), using (3.16) and (3.6) and satisfy the symmetry $\mathcal{K}_\ell(-v_d, c_d) = (-1)^{\ell+1} \mathcal{K}_\ell(v_d, c_d)$.

The case $v_2 \neq 0$ can be studied with a power series in v_2. We prefix a label ^{0} to $\mathcal{K}$ to indicate moments calculated at $v_2 = 0$ and a label ^{2} to indicate the expansion in powers of v_2 as ${}^2\mathcal{K}_\ell = {}^0\mathcal{K}_\ell + (v_2(\ell+2)(\ell+1)\, {}^0\mathcal{K}_{\ell+2})/2 + O(v_2)^2$.

The same considerations apply for the moments of N, defined as $\mathcal{N}_\ell(c_1, v_d, c_d) = \int \mathrm{d}w\, N w^\ell/\ell!$, whose term by term calculation reduces to (B 6).

4. Approximations of integral equation solution

First we study the quasi-equilibrium solution, where j_a is constant, that is $j_{a,z} = 0$; this allows for an electric field, but a constant electric field, that is $v_2 = 0$ everywhere. Then $c_1 = 1$ and $2/\lambda = a_1 c_d$. From (1.1) and § 3 and especially (3.16), we find

$$ \frac{j}{j_a} = 4 \int \mathrm{d}w\, K = 4\, {}^0\mathcal{K}_0 = -v_d c_d \left[1 - \left(\frac{4}{3} + \frac{1}{4} v_d^2 \right) c_d^2 + O(c_d)^3 \right], \tag{4.1} $$

where the series expansion in c_d is the strong recirculation limit and simplifies the long analytic expression of ${}^0\mathcal{K}_0$, given in (B 9). Similarly, from (1.2)

$$ \frac{n_a}{j_a} = \frac{2}{\lambda} \int \mathrm{d}w\, N = \frac{\pi}{v_d} \mathrm{erf} \frac{v_d}{\sqrt{2}} + A_{22}(v_d) c_d^2 + \frac{7\pi(3 + v_d^2)}{12} c_d^3 + O(c_d)^4, \tag{4.2} $$

https://doi.org/10.1017/S0022377815001130 Published online by Cambridge University Press

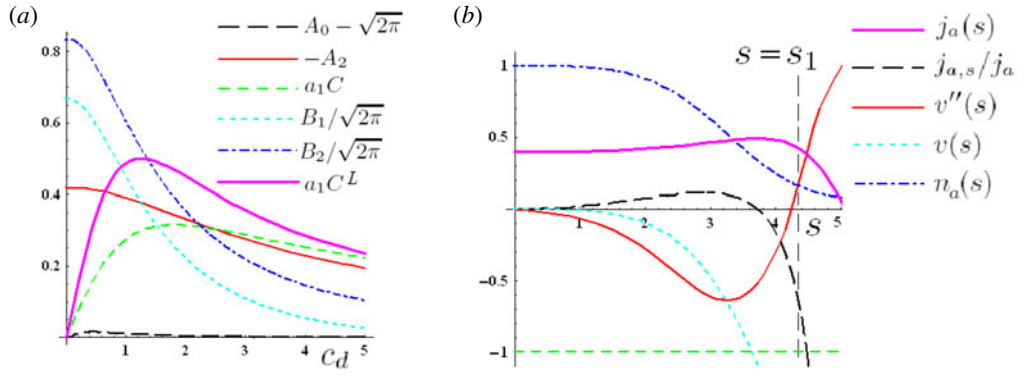


FIGURE 2. (*a*) Density factors $A_0-\sqrt{2\pi}$ and $-A_2$ and $B_1/\sqrt{2\pi}$ and $B_2/\sqrt{2\pi}$ and the conductivity factors a_1C and a_1C^L, as functions of the parameter c_d; (*b*) tracing of $j_a(s)$ solution from (4.7), with $j=0.05$ and $c_d(0)=1.0$; potential $v(s)$ and density $n_a(s)$ and criteria $v''(s)\geqslant -1$ and $|j_{a,s}/j_a|\ll 1$ are also shown.

with coefficient $A_{22}(v_d)\cong\sqrt{2\pi}[(1/3)+(11v_d^2/160)+O(v_d^4)]$. Note that $n_a/j_a\cong\sqrt{2\pi}$ within second-order terms, so that (4.1) shows that current is proportional to $-v_1n_a$; we define a conductivity (in scaled units) as

$$C=-\left(\frac{\partial j/n_a}{\partial v_1}\right)_{v_1=0}=\frac{c_d-c_5c_d^3}{a_1\sqrt{2\pi}}+O(c_d^4)=\frac{(8/\pi)^{1/2}}{a_1c_d}-\frac{8}{\pi a_1c_d^2}+O(c_d^{-3}),\qquad(4.3)$$

where $c_5=5/3$ and we show two expansions of C, one for small c_d values, the other for $c_d\to\infty$ (last step). For all c_d values, the quantity a_1C (which is dimensionless) is shown in figure 2, together with the density factors A_0 and A_2, which are defined by the $n_a/j_a=A_0(c_d)+A_2(c_d)v_d^2+O(v_d^4)$ expansion.

The typical result from fluid equations (Lieberman & Lichtenberg 1994) for the electron mobility μ_e as a function of the collision frequency ν_m (also sometimes referred as a Chapman–Cowling like formula (Tsuda, Fukao & Maeda 1969)) must be represented, in the units used here for conductivity C, as $C^L=\mu_e m v_{th}/e$ where $v_{th}=\sqrt{T_0/m}$, as previously defined. With $\nu_m=k_1v_{th}/\lambda$ and k_1 a numerical factor of approximately one, we find $a_1C^L=2k_1c_d/(4+c_d^2k_1^2)$.

This quantity a_1C^L is plotted in figure 2 with $k_1=(8/\pi)^{1/2}$ (the value for a hard sphere model). Even if C and C^L display similar behaviour for $c_d\to 0$ and $c_d\to\infty$, note that C results up to 40 % less than C^L for intermediate regimes. Corrections to μ_e (and C^L) formula for crossed electric and magnetic fields were proposed elsewhere (Tsuda *et al.* 1969; Daniłko & Barral 2015), with numerical simulations and physical reasoning based on kinetic effects; there, mobility μ_e increases or decreases depending on v_d and electron temperature. In view of the motivations here, following (2.3), we may consider k_1 as an adjustable parameter, which determines λ in terms of the collision frequency ν_m. For the $c_d\to 0$ limit, we obtain $C^L\cong(k_1c_d/a_1)/2$ so that C matches C^L with $k_1=(2/\pi)^{1/2}$. For $c_d\to\infty$, we find $C^L\cong 2/(k_1c_da_1)$ so that C matches C^L with $k_1=(\pi/2)^{1/2}$, which value is not very different from $(8/\pi)^{1/2}$. Whilst further investigations are certainly worthwhile, some partial agreement between C and C^L is already evident.

https://doi.org/10.1017/S0022377815001130 Published online by Cambridge University Press

4.1. *Integral equation for j_a and presheath*

Equation (1.1) can be formally expanded as

$$y(z) \equiv \frac{\lambda}{2} j_{a,z} + \frac{1}{4} j = \int \mathrm{d}w\, K(w; z) j_a(w+z) \cong \sum_{n=0}^{\infty} \mathcal{K}_n j_a^{(n)}(z), \tag{4.4}$$

when the variation of K with z (due to variation of v_0, v_1 and v_2 with z) is much slower than the variation due to w, with the typical scale length L_e, so that the fast w spatial scale can be integrated out. Moments satisfy $\mathcal{K}_n \propto L_e^n \propto (a_1)^{-n}$ from dimensional analysis, so that higher-order derivatives $j_a^{(n)}(z)$ should be bounded by $(\beta_0 a_1)^n$ with a constant $\beta_0 < 1$ for the convergence of sum. This defines the presheath conditions, matching j_a constant at a given $z = z_p$ (which may goes to $-\infty$). By restricting the sum index as $n \leqslant n_T$, with n_T a given integer, we obtain an ODE that can be numerically traced up to some z_0; the region $z \leqslant z_1$ of validity of the solution (depending on n_T and $v(z)$) has to checked case by case, and is smaller than the traced solution: $z_1 < z_0$. We use a combination of criteria $a_1^2 + v_2 > 0$ (which translates to $E_{z,z} > -eB_x^2/m$) and $|j_{a,z}/j_a a_1| < 1$ to estimate z_1; results for the $n_T = 3$ case are shown in examples later.

To improve $\mathcal{K}_n$ convergence, we introduce the so-called regularization technique. Let us define the operators

$$\mathcal{O}_2^z = a - b\partial_z + c{\partial_z}^2, \quad \mathcal{O}_2^w = a + b\partial_w + c{\partial_w}^2 \tag{4.5a,b}$$

and apply $\mathcal{O}_2^z$ to the integral form of (4.4), obtaining

$$\mathcal{O}_2^z y(z) = [K_{,w} j_a + (b j_a - j_{a,z}) K]_{w=-\epsilon}^{w=\epsilon} + \int_{-\infty}^{\infty} \mathrm{d}w\, j_a \mathcal{O}_2^w K(w; z), \tag{4.6}$$

where we consider only the case of a and b constant and $c = 1$ for simplicity, and in the last term (named I_P in the following) the range $R_P \equiv \{-\epsilon < w < \epsilon\}$, with $\epsilon \to 0^+$, is excluded from the integration, similarly to a principal value integral.

Applying the operator $\mathcal{O}_2^z$ to the sum in (4.4), we find

$$\mathcal{O}_2^z y(z) = \frac{1}{4} a j + \frac{\lambda}{2}(a j_a' - b j_a'' + j_a''') = \sum_{n=0}^{\infty} \check{\mathcal{K}}_n j_a^{(n)}(z), \tag{4.7}$$

where the regularized moments are $\check{\mathcal{K}}_n = a\mathcal{K}_n - b\mathcal{K}_{n-1} + \mathcal{K}_{n-2}$ with $\mathcal{K}_{-1} = 0 = \mathcal{K}_{-2}$ for convenience.

If $\mathcal{O}_2^w K(w; z) = 0$, except for the range R_P, (4.6) and (4.7) reduce to differential equations, showing also that $\check{\mathcal{K}}_n = 0$ for $n \geqslant 2$; such simplification can be achieved (Cavenago 2008) for the kernel of the purely electrostatic case, with a first order operator $c = 0$, $b = -v'(z)$ and $a = (v')^2 + \lambda^{-1}|v'| - v''$. In general, $\mathcal{O}_2^w K(w; z) \neq 0$, (4.6) and (4.7) remain integral equations, for which we note some approximate solution methods.

We can simply choose a and b to make $\mathcal{O}_2^w K(w; z)$ much smaller than K, especially in regions $|w| \geqslant L_e$, in order to decrease regularized moments $\check{\mathcal{K}}_n$ for $n > n_T = 3$; in detail a and b are optimized at the initialization of a numerical solver, considering the attenuation lengths of K; then (4.7) is solved, keeping only terms up to $n \leqslant 3$ in the sum; we call this procedure the regularized solver or the (4.7) solution.

https://doi.org/10.1017/S0022377815001130 Published online by Cambridge University Press

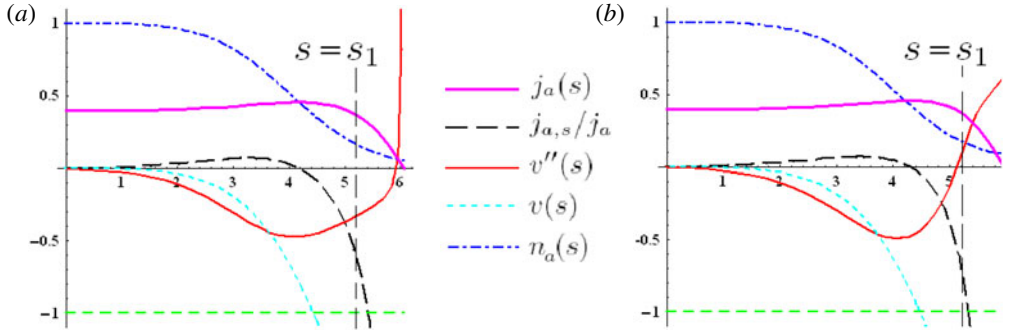


FIGURE 3. (*a*) Solution components as in figure 2(*b*), but with $c_d(0) = 0.5$ and use of (4.4) for j_a; (*b*) same plot with $c_d(0) = 0.5$ and use of (4.7).

4.2. *Coupling to Poisson equation and numerical solutions*

The density expression (1.2) is now expanded, keeping up quadratic terms in $v_d = v_{,z}/a_1$ and ∂_z, and consistently, linear terms in $v_2 = v_{,zz}$; this requires us to include the ${}^2\mathcal{N}_0 j_a = ({}^0\mathcal{N}_0 + {}^0\mathcal{N}_2 v_2) j_a$ terms. Changing coordinate to $s = a_1(z - z_p)$, we write the density

$$n_a = 2\lambda^{-1}[(A_0 + (v_{,s})^2 A_2 + B_2 v_{,ss}) j_a + B_1 v_{,s} j_{a,s} + B_2 j_{a,ss}], \tag{4.8}$$

keeping only the $v_{,s}$ and $v_{,ss}$ dependences explicitly shown; the terms $B_1(c_d)$ and $B_2(c_d)$ which are defined by the expansions ${}^0\mathcal{N}_1 a_1 = v_d B_1 + O(v_d^3)$ and ${}^0\mathcal{N}_2 a_1^2 = B_2(c_d) + O(v_d^2)$ are shown in figure 2(*a*). With the scaled potential $v(z) = -e\phi(z)/T_0$ the Poisson equation becomes

$$(a_1\lambda_D)^2 v_{,ss} = n_{p0} \mathrm{e}^{v(z)} - n_{\mathrm{H}-} - n_{e0} n_a, \tag{4.9}$$

where λ_D is the Debye length and n_{p0} and n_{e0} are constants, depending on plasma equilibrium at $z = z_p$ (deep inside the plasma), which we take as a ground reference $v = 0$. In this analysis, we set $n_{\mathrm{H}-} = 0$, so $n_{e0} = 1 = n_a(0)$ and $n_{p0} = 1$ at $s = 0$; moreover the net flow j (which is a constant parameter under the $\mathcal{S} = 0$ assumption) is set at a small value. For a perfect equilibrium, from (4.3) we see that $v'(0)$ is proportional to j, thus $v'(0) = 0$ is a suitable boundary condition (bc), producing only a short transient near $s = 0$. Other bc are $j_a' = j_a''' = 0$ and $j_a(0)$ as determined by (4.8).

Solutions of the (4.7)–(4.9) system are traced in figures 2 and 3, with a fixed value of the $c_d(0) = 2/(a_1\lambda)$ parameter; in these examples we set $N_0 = 3.2 \times 10^{17}$ m^{-3}, $T_0 =$ 1 eV, $j = 0.05$ (equivalent to $j_e = 1.1$ kA m^{-2}) which are realistic values for intense ion sources. Magnetic flux density B_x is set to 5×10^{-4} T (a low constant value for simplicity), so that $a_1 = 200$ m^{-1}. Two values for λ were considered: $\lambda = 20$ mm (that is $c_d = 0.5$) and $\lambda = 10$ mm that is $c_d = 1.0$; since $\lambda_D = 0.014$ mm and thus $(a_1\lambda_D)^{-2} = 1.3 \times 10^5$ is large, charge quasi-neutrality is satisfied up to approximately z_0 (if charge quasi-equilibrium cannot be maintained, the numerical solution breaks up). The criteria for the (4.4) approximation limits the validity of the solutions, at a $s_1 = a_1(z_1 - z_p)$ shown in figure 3(*a*); similarly for (4.7), see a comparison in figure 3.

Another method of solution, which avoids truncation of sums of $j_a^{(n)}$, is the iterative solution of (4.6): after evaluating the integral term I_P for a trial solution $T_0 = \{j_a(s), v(s), n_a(s)\}$, solving the ODE part of (4.6) gives a new solution T_1; this

https://doi.org/10.1017/S0022377815001130 Published online by Cambridge University Press

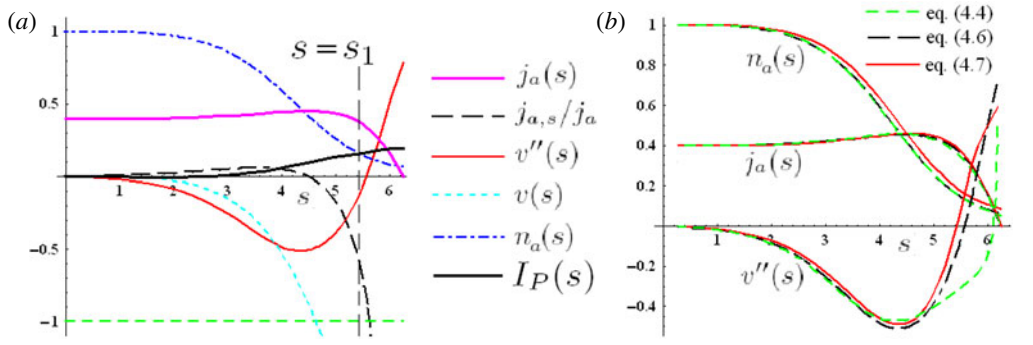


FIGURE 4. (*a*) Solution components as in figure 3(*b*), but with $c_d(0) = 0.5$ and use of iterative solver from (4.6), showing its integral term $I_P(s)$; (*b*) comparison of solution components n_a and $v_{,ss}$ from three solvers, respectively with (4.6), (4.7) and (4.4); axis s origin was shifted to align j_a.

procedure is repeated until convergence (typically slow at 30 iterations, since we require 6 digit stability of the z_0 value). The converged solution is shown in figure 4, including the value of the integral term $I_P(s)$; note that the final value of $I_P(s)$ is small, which helps the convergence of the procedure.

For $s \leqslant s_1$, we note that j_a stays roughly constant, while n_a has to decrease to maintain quasi-neutrality since the proton density decreases with the decrease of potential $v(s)$, and $-v'(s)$ has to increase for consistency with the conservation of j. The $v_{,ss}$ term in (4.8) interacts with the Poisson equation (4.9), with stabilizing effects.

The case of B_x slowly rising towards extraction may be similarly studied.

5. Conclusions, discussion and perspectives

Investigation of a collisional and kinetic model of electron transport in crossed magnetic and electric fields has shown the convenience of expressing the phase density f (a function of two velocities and one space coordinate z) from an absolute flow density j_a, a function of the space coordinate z only as is the number density n_a. With the Poisson equation, the IDE for j_a and n_a make a closed system. Their kernels K and N strongly depend on trapped orbits when the effective Larmor radius L_e is smaller than the mfp λ; suitably approximated analytic formulas were here developed for all $c_d = 2L_e/\lambda$ values, in terms of the error function, including moments of K and N.

When fields are uniform (translation invariance), the IDE can be simply solved, finding a conductivity value that can be compared to the electron mobility from fluid equations.

The methods used for IDE solution with moderate non-uniform fields (presheath) are mainly numerical, and include (best method last): truncation to a third order ODE of (4.4); truncation to a third order ODE of regularized (4.7); and iterative solution of (4.6). The converged solution of (4.6) agrees well with the (4.7) solution, see figure 4(*b*), which so corroborates the use of the regularized solver for a rapid approximated solution of (1.1), (1.2) and (4.9). The criteria $E_{z,z} > -eB_x^2/m$ and $j_a'(z)/a_1 j_a \ll 1$ are required for the presheath, and quasi-neutrality holds in the presheath; note that $E_{z,z}$ (proportional to $v_{,ss}$ plotted in figures) appears not only in the Poisson equation (4.9), but also in the n_a expression (4.8), which mainly determines it.

https://doi.org/10.1017/S0022377815001130 Published online by Cambridge University Press

The presheath solution gives the conditions of the electrons from the plasma, while a different regime ($j_a'(z)/a_1 j_a \ll 1$) holds for the sheath. Matching to fluid models of beam extraction from the sheath is also being investigated.

Appendix A. Integration domains for kernels K and N

In the (2.17) context, a positive w implies that the force $-h_{,z} = pa_{,z}$ has to be non-negative at a reversal point z^-, so $p \geqslant 0$ restricts the domain D^1. Using the θ_C^0 expression, we note that $V_e \geqslant 0$ is required in (2.17), that is $\bar{v} - (\bar{a})^2/2 \geqslant \bar{a}(p + v_d)$. When $w > 0$, it also holds that $\bar{a} < 0$, therefore we require $p > q_1(w) \equiv \max_{w_1 \in [0,w]} q_0(w_1)$, with q_0 defined in (2.18). Assuming reasonable a and v profiles, so that q_0 is a monotonic function of w, then $q_1(w)$ is equal to $q_0(w)$ or to zero. Joining conditions, the domain D^1 is determined by $p \geqslant \max(0, q_0(w))$ for $w > 0$. Similarly, for $w < 0$ we find that D^1 is given by $p \leqslant \min(0, q_0)$. Both expressions join into the $D^1_w(p)$ formula of (2.18).

With respect to the domain D^2, first note that when $z_2 = z^-$ or z^+, we have $\eta_z(z_2) = 0$, that is $p_z^2 + 2V_e(z, z_2) = 0$ or

$$p_z^2 + 2\bar{v} - (\bar{a})^2 - 2\bar{a}(p_y - \bar{a}) = 0, \tag{A 1}$$

with $\bar{a} = a(z) - a(z + w) = -a_1 w$ and $\bar{v} = -v_1 w - v_2 w^2/2$ from (2.19). So

$$w^2 - 2wL_e(p_y - v_d) - p_z^2(L_e/a_1) = 0, \tag{A 2}$$

whose solutions satisfy $w^- \leqslant 0 \leqslant w^+$, for positive L_e/a_1. Second, $P_y^D(z + w) = a_0 + v_d + (w/L_e)$ so that the definitions in (2.21) give $q = w^+/(2L_e)$ and $t = -w^-/(2L_e)$; the conditions for $\theta_C = 1$ that are $z^- \leqslant z \leqslant z^+$ and $z^- \leqslant z_2 \leqslant z^+$ may be translated to $-t \leqslant 0 \leqslant q$ and $-t \leqslant q_0(w) \leqslant q$, so a compact expression of the integration domain is

$$D_w^2(q, t) = \{q \geqslant \max[0, q_0(w)], t \geqslant \max[0, -q_0(w)]\}. \tag{A 3}$$

Third, from (A 2) it follows that

$$q - t = p = p_y - v_d, \quad qt = p_z^2/(4a_1 L_e). \tag{A 4a,b}$$

Moreover, in terms of the parameter $c_d = 2L_e/\lambda$, we have

$$s_d = c_d(q + t), \quad \frac{w}{\lambda} = c_d q_0, \quad \frac{w^+}{\lambda} = c_d q, \quad \frac{w^-}{\lambda} = c_d t. \tag{A 5a–d}$$

Using (A 4), the domain D^2 can be mapped onto the p_z, p_y plane to domains D^b (choosing $\mathrm{sign}(p_z) = -1$)) or D^{fo} (choosing $\mathrm{sign}(p_z) = 1$), whose union is the domain D^3:

$$D_w^3(p_z, p_y) = \left\{ \frac{p_z^2}{4L_e a_1} + [p_y - v_d - q_0(w)]q_0(w) \geqslant 0 \right\}, \quad D^{fo} = D^3 \cap \{p_z \geqslant 0\} \tag{A 6a,b}$$

and $D^b = D^3 \cap \{p_z \leqslant 0\}$, with $\cap$ the intersection.

At any fixed z, we consider a symmetry operation S_1 mapping w onto $-w$, written as $S_1 w = -w$; and $S_1 z_2 = 2z - z_2$. Here, the symmetry group consists only of the identity I and S_1, due to the fact that it is a 1-D model. Representation of S_1 on potentials must be consistent with $S_1^2 = I$, but we can choose signs as follows: $Sv(z + w) \equiv v_S(z + w) = v(z - w)$, $Sa(z + w) \equiv a_S(z + w) = -a(z - w)$ and $S(p_z, p_y) = (-p_z, -p_y)$. In this way, the effective potential V_e expression remains unchanged; moreover $S_1 a_1 = a_1$ (so we need to consider only the case $a_1 > 0$ in all expressions), $S_1 v_2 = v_2$ and $S_1 v_1 = -v_1$. We expect that larger finite symmetry groups may be helpful in 2-D and 3-D models.

https://doi.org/10.1017/S0022377815001130 Published online by Cambridge University Press

Appendix B. Integrations for kernel K and N

Exact values for the (3.5) integral are:

$$f_{1/2}(t_0, s) = \sqrt{\frac{\pi}{2}} \mathrm{e}^{s^2/2} \mathrm{erfc} \frac{s + t_0}{\sqrt{2}}, \tag{B 1}$$

$$f_{3/2}(t_0, s) = \mathrm{e}^{-(1/2)t_0^2 - t_0 s} - s f_{1/2}(t_0, s), \tag{B 2}$$

$$f_{n+1}(t_0, s) = -\partial_s f_n(t_0, s). \tag{B 3}$$

Exact values for $t_0 = 0$ are:

$$f_n(0, s) = 2^{n_1 - 1} \Gamma(n_1)\, {}_1F_1(n_1; \tfrac{1}{2}; \tfrac{1}{2}s^2) - 2^{n_3 - 1} s \Gamma(n_3)\, {}_1F_1(n_3; \tfrac{3}{2}; \tfrac{1}{2}s^2) \tag{B 4}$$

with the shorthand $n_1 = (n/2) + (1/4)$ and $n_3 = (n/2) + (3/4)$, where ${}_1F_1$ is the Kummer confluent hypergeometric function (an expression of (B 4) with Bessel functions is longer).

The leading term for $t_0 \to \infty$ is:

$$f_n(t_0, s) = t_0^{n - (3/2)} \mathrm{e}^{-(1/2)t_0^2 - t_0 s} (1 + O(1/t_0)). \tag{B 5}$$

The partial wave expansion of $\hat{N}$ for the $q_0 = 0$ and $c_1 = 1$ case is:

$$\hat{N}^i_{nk;m}(0;\, 1,\, v_d,\, c_d) \cong \pi \mathrm{e}^{-v_d^2/2} \sum_{i=0}^{n_M} w_i f_{n+(1/2)}(0,\, kc_d + b_i(mc_d + v_d)), \tag{B 6}$$

where n_M is an integer, w_i are weights and b_i are exponents in the following approximation of a modified Bessel function

$$I_0(s) \cong \sum_{i=0}^{n_M} w_i \mathrm{e}^{-b_i s} = \frac{1}{4}[1 + 2\cosh(s/\sqrt{2}) + \cosh s]; \tag{B 7}$$

here the last step is an example with $n_M = 4$, $w_i = 1/4$ except for $w_0 = w_4 = 1/8$; the exponents are $b_4 = -b_0 = 1$, $b_3 = -b_1 = 2^{-1/2}$ and $b_2 = 0$. The (B 6) follows from the observation that in the case $q_0 = 0$, the integration domain D^2 is $q \geqslant 0$ and $t \geqslant 0$, so $s = q + t$ and $p = q - t$ are also convenient coordinates, and in the case $c_1 = 1$ the exponential factor E_1 in (3.7) greatly simplifies, so that

$$\hat{N}^i_{nk;m}(0;\, 1,\, v_d,\, c_d) = \int_0^\infty \mathrm{d}s \int_{-s}^{s} \mathrm{d}p \frac{s^n}{\sqrt{s^2 - p^2}} \mathrm{e}^{-(v_d^2 + s^2)/2 - kc_d s - p(v_d + mc_d)}. \tag{B 8}$$

The integration on p gives $\pi I_0(s(v_d + mc_d))$, which is then approximated by (B 7), with error $O(s^{10})$, whose contribution is suppressed by $\mathrm{e}^{-s^2/2}$, with a maximum error 1.8×10^{-5} around $s = 3$. So the typical relative $e_d(x_d)$ error of (B 6) generally increases with $x_d = |v_d + mc_d| - kc_d$; in detail $e_d(1.) \cong 3 \times 10^{-4}$ and $e_d(2.) \cong 1.2 \times 10^{-2}$ and $e_d \cong 6 \times 10^{-8}$ for $x_d \leqslant 0$, as easily tested in numerical examples.

The rest of the calculations are straightforward. For example, from (3.16), the expression of ${}^0\mathcal{K}_0$ contains terms with $\ell = 0$, $i = \pm 1$, so the denominator c_y takes the values $\pm c_d - 2v_d$ (for integration on the range $w > 0$) and $\pm c_d + 2v_d$. Grouping together terms, we obtain

$${}^0\mathcal{K}_0(v_d, c_d) = \frac{a_{\mathcal{K}}(v_d, c_d)}{2(c_d - 2v_d)} - \frac{a_{\mathcal{K}}(-v_d, c_d)}{2(c_d + 2v_d)}, \tag{B 9}$$

https://doi.org/10.1017/S0022377815001130 Published online by Cambridge University Press

where the coefficient $a_{\mathcal{K}}(v_d, c_d)$ contains 8 occurrences of the erfc function and, defining $h_e(x) = e^{x^2/2}\mathrm{erfc}(x/\sqrt{2})$ and $h_f(x) = xh_e(x)$, it may be more compactly written as

$$a_{\mathcal{K}}(v_d, c_d) = e^{-v_d^2/2}\Big[h_f(c_d + v_d) + h_f(c_d - v_d) - h_f(2c_d - v_d) - h_f(v_d) + (c_e + c_d - v_d)h_e(3c_d - v_d) - (c_e + v_d)h_e(2c_d + v_d) + \frac{h_e(3c_d + v_d) - h_e(4c_d - v_d)}{2c_d}\Big], \quad \text{(B 10)}$$

with the shorthand $c_e = 2c_d + (2c_d)^{-1}$. Note the odd symmetry of (B 9) with respect to v_d and that $a_{\mathcal{K}}(c_d/2, c_d) = 0$, so that ${}^0\mathcal{K}_0$ remains bounded at $v_d = \pm c_d/2$. The expression of ${}^0\mathcal{N}_0(1, v_d, c_d)$ (omitted for brevity) is similar to (B 9), but with even symmetry respect to v_d reflection and a coefficient $a_{\mathcal{N}}(v_d, c_d)$ containing 57 occurrences of erfc function.

REFERENCES

Benilov, M. S. 2009 The Child–Langmuir law and analytical theory of collisionless to collision dominated sheaths. *Plasma Sources Sci. Technol.* **18**, 014005.

Brown, I. G. 2004 *The Physics and Technology of Ion Sources*, 2nd edn. John Wiley & Sons.

Caruso, A. & Cavaliere, A. 1962 The structure of the collisionless plasma-sheath transition. *Nuovo Cimento* **26**, 1389–1404.

Cavenago, M. 2008 Negative ion transport inside collisional presheaths. *Rev. Sci. Instrum.* **79**, 02B709.

Cavenago, M. 2010 Simulations of negative ion plasma sheaths. *Rev. Sci. Instrum.* **81**, 02B501.

Chodura, R. 1982 Plasma–wall transition in an oblique magnetic field. *Phys. Fluids* **25**, 1628–1633.

Daniłko, D. & Barral, S. 2015 Contribution of phase-energy correlation to classical mobility across a strong magnetic field. *Phys. Scr.* **90**, 055601.

Dikman, S. M. & Meierovich, B. E. 1973 Theory of the anomalous skin effect in a plasma with a diffuse boundary. *Sov. Phys. JETP* **37**, 835–843.

Emmert, G. A., Wieland, R. M., Menzel, A. T. & Davidson, J. N. 1980 Electric sheath and presheath in a collisionless, finite ion temperature plasma. *Phys. Fluids* **23**, 809–812.

Forrester, A. T. 1996 *Large Ion Beams*. Wiley.

Franklin, R. N. 2003 The plasmasheath boundary region. *J. Phys.* D **36**, R309–R320.

Hutchinson, I. H. 1987 A fluid theory of ion collection by probes in strong magnetic fields with plasma flow. *Phys. Fluids* **30**, 3777–3781.

Lieberman, M. A. & Lichtenberg, A. J. 1994 *Principles of Plasma Discharges and Material Processing*. Wiley, especially Table 3.1 at page 57 and eq. (5.4.4) at page 142.

Mochalskyy, S, Lifschitz, A. F. & Minea, T. 2010 3D modelling of negative ion extraction from a negative ion source. *Nucl. Fusion* **50**, 105011.

Morse, P. M. & Feshbach, H. 1953 *Methods of Theoretical Physics*. McGraw-Hill, especially chap. 8.

Riemann, K. U. 1991 The Bohm criterion and sheath formation. *J. Phys.* D **24**, 493–518.

Schmitz, H., Riemann, K. U. & Daube, Th. 1996 Theory of the collisional presheath in a magnetic field parallel to the wall. *Phys. Plasmas* **3**, 2486–2495.

Self, S. A. 1963 Exact solution of the collisionless plasma–sheath equation. *Phys. Fluids* **6**, 1762–1768.

Taccogna, F., Schneider, R., Longo, S. & Capitelli, M. 2008 Modeling of surface-dominated plasmas: from electric thruster to negative ion source. *Rev. Sci. Instrum.* **79**, 02B903.

Taccogna, F., Minelli, P. & Longo, S. 2013 Three-dimensional structure of the extraction region of a hybrid negative ion source. *Plasma Sources Sci. Technol.* **22**, 045019.

https://doi.org/10.1017/S0022377815001130 Published online by Cambridge University Press

TAKADO, N., MIYAMOTO, K. & HATAYAMA, A. 2004 Numerical modeling of excited hydrogen atoms and their transport in hydrogen negative ion sources. *Rev. Sci. Instrum.* **75**, 1777–1779.
TONKS, L. & LANGMUIR, I. 1929 General theory of the plasma of an arc. *Phys. Rev.* **34**, 876–922.
TSUDA, T., FUKAO, S. & MAEDA, K. 1969 Gyromagnetic effect on the mobility of charged particles in weakly ionized gases. *J. Appl. Phys.* **40**, 5280–5289.
Wolfram Mathematica®, www.wolfram.com; see also S. Wolfram 2003 *The Mathematica Book, 5th edn.*, Champaign: Wolfram Media, especially for Series and NDSolve descriptions.

https://doi.org/10.1017/S0022377815001130 Published online by Cambridge University Press